J|A|C|S
ARTICLES
Published on Web 02/23/2007

DNA−Protein Interactions as the Source of Large-Length-Scale Chirality Evident in the Liquid Crystal Behavior of Filamentous Bacteriophages

Sonit Tomar,[†,‡] Mark M. Green,*[,†] and Loren A. Day*[,‡]

Contribution from the Department of Chemical and Biological Sciences, Polytechnic University, Brooklyn, New York 11201, and the Public Health Research Institute, Newark, New Jersey 07103

Received November 27, 2006; E-mail: mgreen@duke.poly.edu; day@phri.org

Abstract: Although all filamentous phages are constructed of chiral components, this study of eight of these phages (fd, IKe, $I_2$2, X-2, Pf1, Pf3, tf-1, and X) shows that some form nematic liquid crystals, which are apparently oblivious to the chirality of the components, while others form cholesteric liquid crystals revealing a type of structural chirality not normally encountered. Additions of dopants that interact with the DNA or protein components of the viruses change the liquid crystal properties of seven of the phages. In these seven, DNA−capsid symmetry differences do not allow strict structural equivalency among the protein subunits. The polymorphism arising from this nonequivalency is proposed here to give rise to coiling of the filaments, a large-length-scale chirality that is responsible for forming cholesteric liquid crystal phases. Only one phage of those studied here, Pf1, which is distinguished from the others in its DNA−capsid interactions, forms nematic phases under all conditions tried. The formation of liquid crystals has been developed as a method to detect subtle overall shape effects arising from DNA-subunit-derived polymorphism, an unusual role for the mesogenic state and a new tool for the study of filamentous phage structure.

Introduction

Filamentous bacteriophages contain circular single-stranded DNA genomes that extend from one end of their virions to the other and back again within capsid shells made of thousands of chemically identical protein subunits.[1−6] Many strains are known,[2] and some of the phage/host systems are plant and animal pathogens, including one that carries the toxin genes causing cholera, the devastating disease of humans.[3] These phages all have diameters of only about 7 nm, but their contour lengths range from 700 nm to over 2000 nm depending on the size and conformation of the DNA that is packaged.[4] The packaging occurs at the bacterial membranes as the virions are extruded into the medium.[5,6]

Fraden and co-workers investigated solutions of fd and Pf1,[7,8] two widely studied phages, and found concentration-dependent spontaneous formation of liquid crystals in accord with the Onsager theory of such entropy-driven phase separations.[9] However, the studies yielded a surprise in that Pf1 exhibited the classic birefringence of a nematic phase, in which the viral particles are approximately parallel to each other, while fd formed a cholesteric liquid crystal phase, one in which the ensemble of approximately parallel viral particles forms a helical array. Since both fd and Pf1 are made of similar chiral components arranged in similar ways, one is surprised at the absence of a cholesteric phase in Pf1. To explain the difference in their liquid crystal phases, Grelet and Fraden[8] report that R. B. Meyer, in a private communication, has hypothesized that fd has the overall shape of a gentle coil or corkscrew yielding handedness on a large length scale, which was seen as necessary to form the cholesteric phase.

Normally the local chiralities of individual components of a liquid crystal forming entity (a mesogen) including the configurations around asymmetric carbon atoms, the secondary structures of proteins, polysaccharides, or nucleic acids, and, at the next higher structural level, chirality in the arrangements of near neighbors in larger assemblies are sufficient to enforce cholesteric phases in liquid crystals.[10,11] These levels of local chirality are transmitted between mesogens by steric or electrostatic interactions to generate cholesteric phases in liquid

[†] Polytechnic University.
[‡] Public Health Research Institute.

(1) Marvin, D. A. *Curr. Opin. Struct. Biol.* **1998**, *8*, 150−158.
(2) Day, L. A.; Hendrix, R.W. In *Virus Taxonomy. Eighth Report of the International Committee on the Taxonomy of Viruses*; Fauquet, C. M., et al., Eds.; Elsevier Academic Press: New York, 2005; pp 279−287.
(3) Davis, B. M.; Waldor, M. K. *Curr. Opin. Microbiol.* **2003**, *6*, 35−42.
(4) Day, L. A.; Marzec, C. J.; Reisberg, S. A.; Casadevall, A. *Annu. Rev. Biophys. Biophys. Chem.* **1988**, *17*, 509−539.
(5) Model, P.; Russel, M. In *The Bacteriophages*, 2nd ed.; Calendar, R., Ed.; Oxford University Press: Oxford, U.K., 2006.
(6) Webster, R. E. In *Phage Display of Peptides and Proteins*; Kay, B. K., Winter, J., McCaffery, J., Eds.; Academic Press: New York, 1996; pp 1−20.
(7) Dogic, Z.; Fraden, S. *Langmuir* **2000**, *16*, 7820−7824.
(8) Grelet, E.; Fraden, S. *Phys. Rev. Lett.* **2003**, *90*, 198302.
(9) Onsager, L. *Ann. N. Y. Acad. Sci.* **1949**, *51*, 627−659.
(10) Chandrasekhar, S. *Liquid Crystals*, 2nd ed.; Cambridge University Press: Cambridge, U.K., 1992.
(11) Green, M. M.; Zanella, S.; Gu, H.; Sato, T.; Jha, S. K.; Spada, G. P.; Scoevaars, A. M.; Feringa, B.; Teramoto, A. *J. Am. Chem. Soc.* **1998**, *120*, 9810−9817 and references therein.

10.1021/ja068498d CCC: $37.00

Table 1. Major Coat Protein Sequences of Eight Filamentous Phages[a]

Phage	Domains Solvent Interaction — DNA Interaction	Virion Length (nm)
fd(Ff)	AEGDDPAKAAFDSLQASATEYIGYAWAMVVVIVGATIGIKLFKKFTSKAV	890
IKe	AEPNAATNYATEAMDSLKTQAIDLISQTWPVVTTVVVAGLVIRLFKKFSSKAV	1100
$I_2$2	ADDGTSTATSYATEAMNSLKTQATDLIDQTWPVVTSVAVAGLAIRLFKKFSSKAV	1050
X-2	EGTTTNTDYAGQAMTELLTQANDLIGKVWPVVVAVVGAALAIRLFKKFSSKAV	950
Pf1	GVIDTSAVESAITDGQGDMKAIGGYIVGALVILAVAGLIYSMLRKA	2100
Pf3	MQSVITDVTGQLTAVQADITTIGGAIIVLAAVVLGIRWIKAQFF	720
tf-1	MGTTNTLVSMVNGVDLSDMNSAVLAAGGLMLGAAVALMGIRRVIRMFKG	850
X	AEGDVVGGKGIDLTPLTNSVNFGSVLTGIMAVAGSLIVLYAGSAGVRWILRMVRGA	1255

[a] Capsid protein sequences are from Genbank except those for X-2 (unpublished result of Lena Wong and L.A.D) and for tf-1 and X (unpublished results of J. Kota, R. Donnelly, S.T., and L.A.D). In the extensively studied Ff group of fd, f1, and M13, the sequences of f1 and fd are the same but that of M13 has N (asn) at position 12. Virion contour lengths[4] are from scanning transmission electron microscopy and/or hydrodynamics in collaboration with J. S. Wall and J. Newman, respectively. The measurements for $I_2$2, X-2, tf-1, and X will be reported separately. The numbers of subunits in the virions range from about 2300 for Pf3 to about 7300 for Pf1.

crystals. However, the calculated average distance between filamentous phage particles in the concentration range within which cholesteric phases are observed, 10−100 mg/mL, lies between about 20 and 70 nm. These distances correspond to about 10 virion diameters at the lower concentrations down to 3 diameters at the higher concentrations in the high ionic strength buffers that screen electrostatic interactions, so it is understandable that local chiralities are not transmitted in such solutions. The necessity, therefore, for chirality on a large length scale to explain the cholesteric phases is reinforced by the long-known absence of a cholesteric phase in tobacco mosaic virus, which is clearly chiral on local length scales of its structure. Moreover, the idea of coiling, a prerequisite for a large-length-scale chirality, in the filamentous phage fd is reasonable in that preexisting electron microscopic images of other filamentous phages, C2[12,13] and X,[14] suggest regular periodicities superimposed on randomly flexed filaments. However, accepting the hypothesis of coiling in fd leaves unanswered the question of why Pf1 does not show a cholesteric liquid crystal phase. Why should large-length-scale chirality be present in fd but not be present in Pf1?

In an attempt to answer this question, we have reexamined fd and Pf1 under a variety of conditions and have studied six additional filamentous phages for further comparisons. The eight phages are listed in Table 1. All eight are similar in that the capsid protein subunits are about the same size (50 ± 6 amino acids), are highly α-helical, and have acidic N-terminal domains, hydrophobic central domains, and basic C-terminal domains. In the capsids the subunits overlap and interdigitate with each other so that the α-helices are approximately parallel to the main axes of the virions. The C-terminal domains interact with DNA and the N-terminal domains with solvent. The positive charges of the C-domains approximately balance DNA phosphate charges, giving the virions about the same negative linear charge density of −1 e/Å at neutral or slightly alkaline pH.

Given these overall similarities, we hypothesized that differences in liquid crystal behavior might be related to differences between the helical symmetries of the capsids and the packaged DNA genomes. With respect to the capsids, two general types or classes of helical symmetry have been observed. X-ray fiber diffraction patterns and physicochemical data for the top four viruses in the table (fd, IKe, $I_2$2, and X-2) indicate the individual protein subunits are arranged around the DNA in pentamers that overlap with neighboring pentamers. The entire capsid is generated by successive pentamer translations of 16−17 Å and pentamer rotations of approximately 36°, so that there are approximate repeats every 32−34 Å.[15−17] This is referred to as class I symmetry. Class II symmetry is defined by X-ray fiber diffraction data for Pf1 and Pf3 that show subunits related by successive monomer translations and rotations of about 3 Å and 67°, respectively.[15,18−23] Capsid symmetries for tf-1 and X have not been determined, but on the basis of subunit packing theory[21] and sequence comparisons they are expected to be of the class II type. Diagrams of class I and class II capsid symmetries are provided in refs 15 and 21.

The differences in DNA structure are immediately evident in the values for the average rise per nucleotide obtained by dividing virion contour lengths by half the number of nucleotides in the DNA. The nominal values are 2.8 Å for fd, 3.0 Å for $I_2$2, IKe, and X2, 5.8 Å for Pf1, 2.4 Å for Pf3, 2.5 Å for tf-1, and 3.2 Å for X.[4,24] For comparison, the value for classical B-form DNA is 3.4 Å, that of A-form DNA is 2.6 Å, and that of P-form DNA is 5.9 Å.[25] Extensive spectroscopic results together with topological and electrostatic constraints indicate

(12) Bradley, D. E.; Sirgel, F. A.; Coetzee, J. N.; Hedges, R. W.; Coetzee, W. F. *J. Gen. Microbiol.* **1982**, *128*, 2485−2498.
(13) Kostrikis, L. G.; Reisberg, S. A.; Kim, H. Y.; Shin, S.; Day, L. A. *Biochemistry* **1995**, *34*, 4077−4087.
(14) Bradley, D. E.; Coetzee, J. N.; Bothma, T.; Hedges, R. W. *J. Gen. Microbiol.* **1981**, *126*, 389−396.
(15) Caspar, D. L.; Makowski, L. *J. Mol. Biol.* **1981**, *145*, 611−617.
(16) Marvin, D. A.; Hale, R. D.; Nave, C.; Helmer-Citterich, M. *J. Mol. Biol.* **1994**, *235*, 260−286.
(17) Wang, Y. A.; Yu, X.; Overman, S.; Tsuboi, M.; Thomas, Jr., G. J.; Egelman, E. H. *J. Mol. Biol.* **2006**, *361*, 209−215.
(18) Marvin, D. A.; Wiseman, R. L.; Wachtel, E. *J. Mol. Biol.* **1974**, *82*, 121−138.
(19) Wiseman, R. L.; Day, L. A. *J. Mol. Biol.* **1977**, *116*, 607−611.
(20) Peterson, C. W.; Winter, W. T.; Dalack, G. W.; Day, L. A. *J. Mol. Biol.* **1982**, *162*, 877−881.
(21) Marzec, C. J.; Day, L. A. *Biophys. J.* **1988**, *53*, 425−440.
(22) Liu, D. J.; Day, L. A. *Science* **1994**, *265*, 671−674.
(23) Welsh, L. C.; Symmons, M. F.; Sturtevant, J. M.; Marvin, D. A.; Perham, R. N. *J. Mol. Biol.* **1998**, *283*, 155−177.
(24) Tomar, S. Ph.D. Thesis, Polytechnic University, Brooklyn, NY, 2006.
(25) Allemand, J. F.; Bensimon, D.; Lavery, R.; Croquette, V. *Proc. Natl. Acad. Sci. U.S.A.* **1998**, *95*, 14152−14157.

that the eight DNA helices are of only two broadly defined types, bases in and bases out. The DNA helices in fd, IKe, $I_2$2, X-2, tf-1, and X are right-handed helices with pitches near 30 Å and with stacked bases directed in, away from the capsid, as discussed further below.[4,26−28] These pitches differ from those of their surrounding capsids. In contrast, the DNA helices of Pf1 and Pf3 are proposed to share the approximately 16 Å pitches of their respective capsids and to have unstacked bases directed out, toward the capsid.[4,19,22,26−28]

Experimental Section

Bacteriophages and their Bacterial Hosts. The eight strains of phages and their host bacteria used were standard wild types.[2] Filamentous virus fd belongs to a group of closely related viruses (f1, fd, M13) that infect male (F^+ and Hfr) strains of *Escherichia coli* carrying incompatibility group F (incF) elements. IKe, $I_2$2, and X-2, the three viruses with extensive sequence homologies to fd and to each other as listed in Table 1, infect *E. coli* strains bearing incN elements (IKe), bearing $IncI_2$ elements ($I_2$2), and bearing IncX elements (X-2). Pf1 and Pf3 infect *Pseudomonas aeruginosa* strains K (PAK) and O1 (PAO1), respectively. Filamentous virus tf-1 infects *E. coli* harboring the IncT plasmid pIN25, and X infects *E. coli* bacteria harboring the IncX plasmid R6K. Standard methods were used for virus growth and purifications, including equilibrium banding in CsCl density gradients. Luria−Bertani medium, top agar, and agar plates were used for the growth and infectivity assays in all eight systems. Stocks of tf-1, X-2, and X phages and their hosts were received from D. E. Bradley (St. Johns University, Newfoundland, Canada). Genomic sequencing and physical characterizations of tf-1, X-2, and X have been done in collaboration with R. F. Donnelly (New Jersey Medical School, Newark, NJ), J. Newman (Union College, Schenectady, NY), and J. S. Wall (Brookhaven National Laboratory, Upton, NY) and will be reported separately.

Spectroscopic Methods. The virus concentrations were based on UV spectra recorded from 350 to 230 nm with CARY 219, CARY 300, and CARY 50 spectrophotometers from the Varian Corp. The specific absorbance coefficients at wavelength maxima were 3.84 A mg^{-1} cm^2 at 269 nm for fd, 3.5 A mg^{-1} cm^2 at 272 nm for Ike, 3.5 A mg^{-1} cm^2 at 270 nm for $I_2$2, 3.5 A mg^{-1} cm^2 at 270 nm for X-2, 2.1 A mg^{-1} cm^2 at 271 nm for Pf1, 4.5 A mg^{-1} cm^2 at 262 nm for Pf3, 2.9 A mg^{-1} cm^2 at 258 nm for tf-1, and 2.9 A mg^{-1} cm^2 at 268 nm for X. These coefficients include modest light scattering contributions to the apparent absorbance of these filamentous structures and are the current best estimates based on extinction coefficients of component chromophores and absorbance measurements on disrupted virions. Values for fd, Pf1, Pf3, and IKe are available in the literature.[4] Circular dichroism (CD) spectra were recorded on a JASCO J-710 spectropolarimeter calibrated with d_{10}-camphorsulfonic acid. The samples were maintained at 25 °C in water-jacketed quartz cells.

Liquid Crystal Techniques. For each of the eight viruses, sealed quartz capillaries were prepared to contain approximately 10 μL of virus solutions at several concentrations ranging from 10 to 125 mg/mL. The buffer was 0.15 M sodium borate (pH 8.6), a buffer that has good UV transparency, as well as soluble salts with Ag^+ and Hg^{2+} ions, a pH well above the isoelectric points of the viruses yet below the p*K* values of weakly basic lysines and tyrosines, and an ionic strength sufficient to make negligible ionic strength effects on liquid crystal formation[8] and sufficient to buffer the protons displaced on binding of the metal ions to the DNA in the virions[26−29] (phage concentrations of 100 mg/mL have nucleotide concentrations of 0.02−0.05 M, depending on the strain). The capillaries were of nominal 0.7 mm outer diameter (Charles Supper Co., Natick, MA). To prepare samples, buffered virus solutions in the 10 mg/mL range were centrifuged at 200,000 G to yield thick pellets of 150−200 mg/mL. Virus concentrations in these pellets were determined from UV absorbance spectra of weight/volume dilutions of 3−4 mg of pellets in 1 mL of buffer. Dilutions of the pellets were made by weight into the 10−100 mg/mL range for the formation of liquid crystals. Approximately 10 μL of each solution was drawn into a capillary which was then flame sealed at one end. Centrifugation at low speed moved the concentrated virus solution to this sealed end, after which the other end was flame sealed under reduced pressure to prevent microfissures in the seal.

For studies of the effects of Ag^+ and Hg^{2+} ions, quantities of $AgNO_3$ or $HgCl_2$ were added to yield different ratios of moles of metal ion per mole of nucleotide in the intact virions (M_{Ag}/M_{Nu} or M_{Hg}/M_{Nu}). The additions were made prior to the pelleting of the virus. Dissociation of the metal ions from the virions on resuspension of the metal ion−virus complexes in the pellet was minimal because of the high overall concentrations and the high affinity of silver ions for the DNA.[26−29] For studying the effects of added sodium dodecyl sulfate (SDS), weight dilutions of stock pellets were made into buffer already containing SDS at the desired concentrations to prevent any exposure of virus to high local concentrations of SDS. Several hundred sealed capillaries were produced over the course of the entire study. Infectivity assays showed that Ag−virus complexes, Hg−virus complexes, and SDS−virus complexes described in this paper were fully infectious.

The sealed capillaries were left at room temperature and examined at various times by polarized light microscopy with a Nikon Optiphot2-POL microscope with white light from a tungsten source under a 4× magnifying lens equipped with a Nikon Coolpix-5400 digital camera. The liquid crystal textures were observed with capillaries at approximately 45° with respect to the crossed polarizers. The line spacings of the cholesteric fingerprint patterns, which equal half the cholesteric pitch, were measured by photographing a standard microscope ruler with the patterns and analyzing the data with NIH Image 1.6.0 version software. Initially the solutions were isotropic and therefore did not transmit light through the crossed polarizers. Within a few hours samples above minimum concentrations for the isotropic−anisotropic phase transitions specific for each virus began yielding patterns of birefringence typical of liquid crystals. We observed a complex interplay between the curved capillary surface and the developing liquid crystal phase. In the samples we assigned as cholesteric phases, we first observed random orientations of fingerprint patterns, which slowly changed to the more uniform patterns seen in the figures. Next to the sealed end in contact with the liquid crystal solution a less uniform fingerprint pattern was maintained. This observation and the assignment of a cholesteric phase are in agreement with Fraden and co-workers[7,8] in their assignment of a cholesteric phase to fd virus.

Results

Liquid Crystal Behavior of Eight Filamentous Phages. Figure 1 shows birefringence patterns from polarized microscopy that are typical for each of the eight viruses. Three viruses (fd, Pf3, and tf-1) formed the classic fingerprint pattern of cholesteric phases, while four others (IKe, $I_2$2, X-2, and Pf1) exhibited nematic patterns. Phage X formed a gel-like state. The results in Figure 1 are surprising in view of the many structural data that characterize these viruses as summarized in the Introduction, and especially so in pairwise comparisons between fd and IKe and between Pf1 and Pf3. As described in the Introduction, within the first pair the capsid structures are both class I and the DNAs are of the bases-in type, while in the second pair the

(26) Casadevall, A.; Day, L. A. *Nucleic Acids Res.* **1982**, *10*, 2467−2481.
(27) Casadevall, A.; Day, L. A. *Biochemistry* **1983**, *22*, 4831−4841.
(28) Day, L. A.; Casadevall, A.; Prescott, B.; Thomas, G. J., Jr. *Biochemistry* **1988**, *27*, 706−711.
(29) Arakawa, H.; Neault, J. F.; Tajmir-Riahi, H. A. *Biophys. J.* **2001**, *81*, 1580−1587.

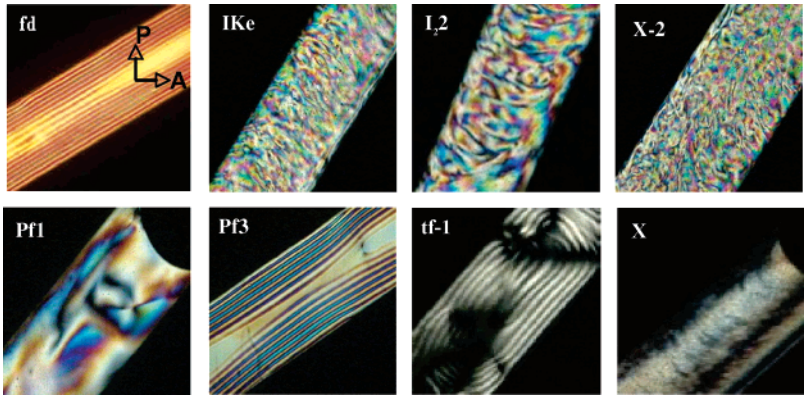

Figure 1. Liquid crystalline solutions of seven viruses and a gel of one virus in capillaries viewed by polarized light microscopy after stable birefringence textures were obtained. The positions of the polarizer (P) and analyzer (A) are indicated in the upper right corner of the panel for fd. Virus concentrations were the minimum concentrations at which birefringent patterns appeared for each virus, namely, 20 mg/mL for fd, IKe, $I_2$2, and X-2, 15 mg/mL for Pf1, 50 mg/mL for Pf3, 25 mg/mL for tf-1, and 75 mg/mL for X (gel pattern). The buffer was 0.15 M borate buffer (pH 8.6). The capillary diameters were nominally 0.7 mm. The edge lengths of the squares correspond to an actual length of 1.5 mm.

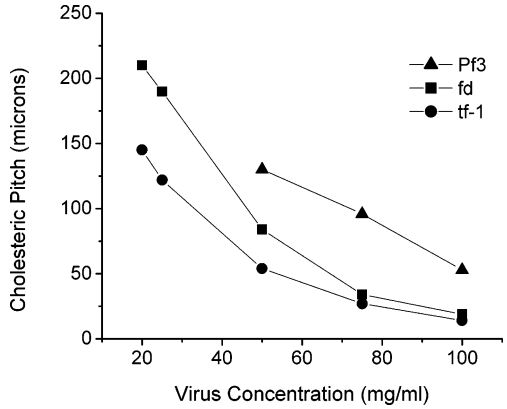

Figure 2. Dependence of the cholesteric pitch, *P*, on concentration for tf-1, fd, and Pf3 viruses. The first concentration shown for each virus is the concentration at which the liquid crystal phase first appears.

capsid structures are both class II and the DNAs are proposed to be of bases-out type, yet one virion of each pair yields a nematic phase and the other a cholesteric phase. Neither of these results was expected.

The separations between the lines in the fingerprint patterns for cholesteric phases are equal to 1/2 the cholesteric pitches, and, as expected for lyotropic cholesteric liquid crystals,[7,8,10] these pitches decrease with increasing virus concentration as shown in Figure 2 for the three viruses which give cholesteric phases in the absence of dopants (fd, Pf3, and tf-1).

Effects of Ag^+ and Hg^{2+} Ions. The liquid crystal patterns of Figure 1 change in the presence of metal ions that bind directly to the DNA and in the presence of SDS that binds directly to the protein. We used low concentrations of dopants that did not affect phage infectivity. The dopants Ag^+ and Hg^{2+} reversibly displace protons from the bases of DNA in filamentous phages, producing changes in the ultraviolet absorbance and CD spectra[26,27] and specific residue changes in the Raman spectra.[28] The changes are readily seen in ultraviolet spectra above 250 nm where the contributing chromophores are the

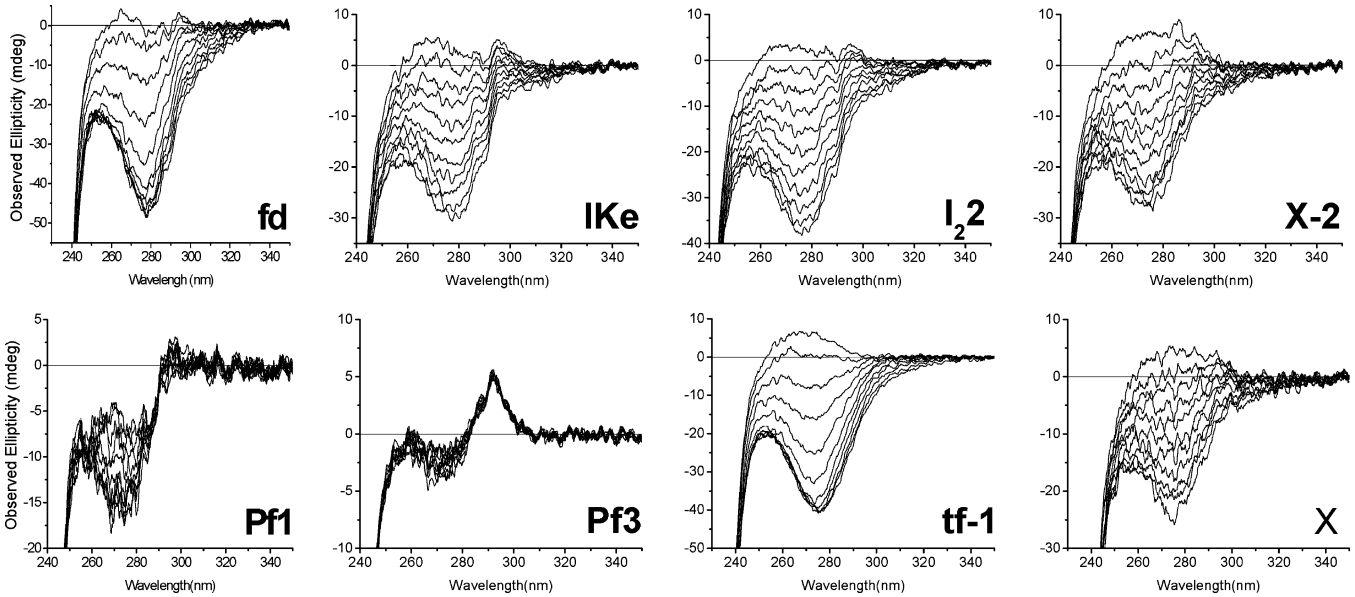

Figure 3. CD monitoring of Ag^+ titrations of eight filamentous phages in the spectral region above 250 nm. The path lengths were 10 mm, and the virus concentrations were approximately 0.2 mg/mL. In all cases, the uppermost spectrum is that for the virus in the absence of added Ag^+ ions, and the successive spectra downward are for successive increments of 0.10 in the ratio of silver ions to nucleotides, M_{Ag}/M_{Nu}. The spectra for the sixth increments are for $M_{Ag}/M_{Nu} = 0.6$, which is the mole ratio in the liquid crystals of Figure 4. These CD spectra were obtained at 100−300-fold lower total concentrations than those in the liquid crystals.[24,26,27]

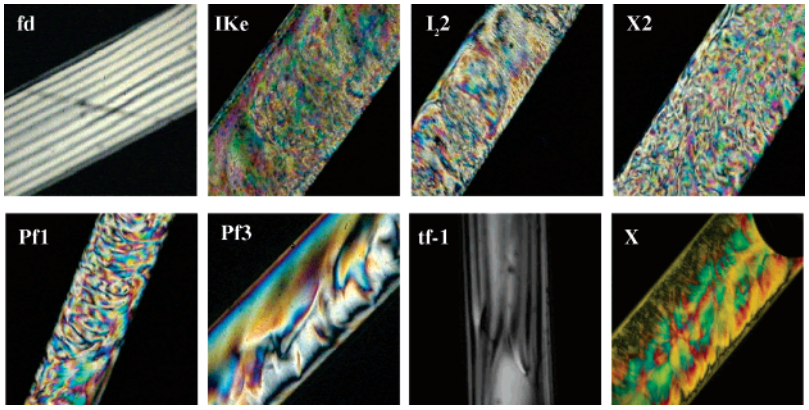

Figure 4. Liquid crystal phases of the eight viruses at mole ratios of 0.6 Ag^+ ion per nucleotide. Virus concentrations were 25 mg/mL for all, except for Pf3 (50 mg/mL) and X (75 mg/mL). For Pf3, a mole ratio of only 0.3 Ag^+ ion per nucleotide converted the cholesteric phase to a nematic phase.

aromatic protein side chains and the DNA bases, and the changes are characteristic of ions binding to DNA bases in either stacked or unstacked conformations.

The CD results for titrations with Ag^+ are presented in Figure 3. They reproduce earlier work on fd, IKe, Pf1, and Pf3[26,27] and extend such observations to $I_2$2, X2, tf-1, and X.[24] CD spectra recorded below 250 nm (not shown) revealed no changes assignable to any changes in protein structure, in accord with previous studies.[26,27] Ag^+ ion titrations of covalently closed circular duplex DNA molecules (supercoiled duplex DNA), in which the right-handedness of the fundamental Watson−Crick base-paired DNA helix is topologically locked in, produce CD changes closely similar to those shown in Figure 3 for fd, IKe, $I_2$2, X-2, tf-1, and X.[26,27] The virtual congruence of the CD results for these six virions and for supercoiled DNAs establishes that the antiparallel single-stranded portions of the loops of circular DNA in the virions constitute right-handed, base-stacked helices with pitches near 30 Å and bases pointing inward. Thus, the DNA helices in fd, IKe, $I_2$2, X-2, tf-1, and X are all similar to base-paired duplex DNA, even though only about 25% of the bases in the opposite strands can H-bond in Watson−Crick-type pairs. By contrast, the CD spectra for the Ag^+-doped Pf1 and Pf3 virions, which reproduce earlier measurements on these viruses,[26,27] demonstrate again that these two DNAs differ greatly in their structures from the DNAs in fd and IKe.

As shown in Figure 4, we found that the four viruses exhibiting nematic phases in the absence of Ag^+ (Pf1, IKe, $I_2$2, and X-2) maintained these nematic phases in the presence of Ag^+. The three viruses that exhibited cholesteric phases in the absence of Ag^+ (fd, Pf3, and tf-1) showed substantially increased cholesteric pitch as the proportion of silver ion increased, even leading to the observation of a nematic phase. As an example, Figure 5 shows the increases in cholesteric pitch for fd at various virus concentrations as functions of the ratio of silver ions to nucleotides, M_{Ag}/M_{Nu}. Note that the presence of 1.2 mol of Ag^+ per nucleotide actually prevented liquid crystal formation at 20 mg/mL fd virus and produced nematic liquid crystals at 25 mg/mL virus, whereas in the absence of silver ions cholesteric liquid crystals are observed at both of these virus concentrations (Figure 2, uppermost points).

The effects of silver ion on the cholesteric pitches of Pf3 and tf-1 were similar to those for fd, although for Pf3 a low M_{Ag}/M_{Nu} ratio of only 0.3 produces nematic liquid crystals (Figure 4). Note that the gel-like pattern for X in Figure 1 was

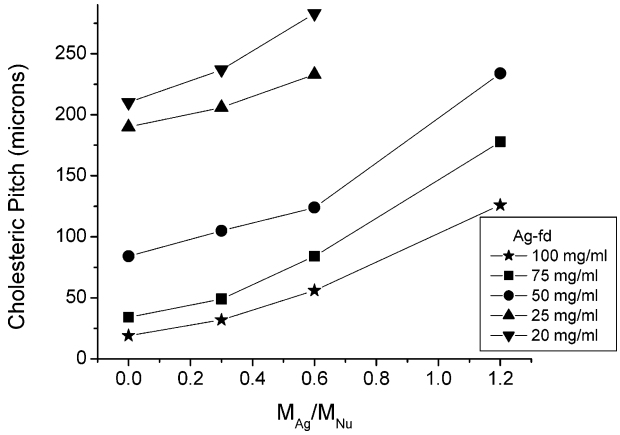

Figure 5. Variation of the cholesteric pitch of fd liquid crystals at five virus concentrations as a function of the mole ratio of added Ag^+ per nucleotide, M_{Ag}/M_{Nu}. At 20 mg/mL virus and $M_{Ag}/M_{Nu} = 1.2$, a liquid crystal did not form. At 25 mg/mL virus and $M_{Ag}/M_{Nu} = 1.2$, the liquid crystal phase was nematic. A similar plot characterizes tf-1 behavior, but the initially cholesteric Pf3 liquid crystals become nematic at $M_{Ag}/M_{Nu} = 0.3$, which was the lowest mole ratio tried.

transformed to a nematic pattern in the presence of Ag^+ ions (Figure 4). Additions of mercury ions affected liquid crystal behavior in ways parallel to those of silver ions for all eight viruses. When silver and mercury ions bind to the DNAs in these viruses, they reversibly displace protons from the bases, with dissociation constants on the order of 10^{-5}.[26−29]

Effect of SDS. In stark contrast to the effect of the metal ions, the presence of low concentrations of SDS in the liquid crystal solutions led to tightened pitches of cholesteric phases and even to conversions of nematic to cholesteric behavior for three of the viruses (Figures 6 and 7). The effects of SDS on the liquid crystal behavior are presented as functions of both M_{SDS}/M_{Su}, the ratio of the total moles of SDS and subunits present, and the weight/volume concentration of SDS (%).

As shown in Figure 6, we observed that as little as one SDS molecule per fifty protein subunits was capable of causing easily observable effects on the liquid crystals. This observation demonstrates high levels of cooperativity in these systems. Apparently a small number of SDS molecules per virion can affect its structure and shape, leading to changes in the transmission of the chiral information necessary to affect the cholesteric states. As a quantitative example of how the presence of SDS tightens the cholesteric pitches, Figure 7 shows the results for $I_2$2 liquid crystals.

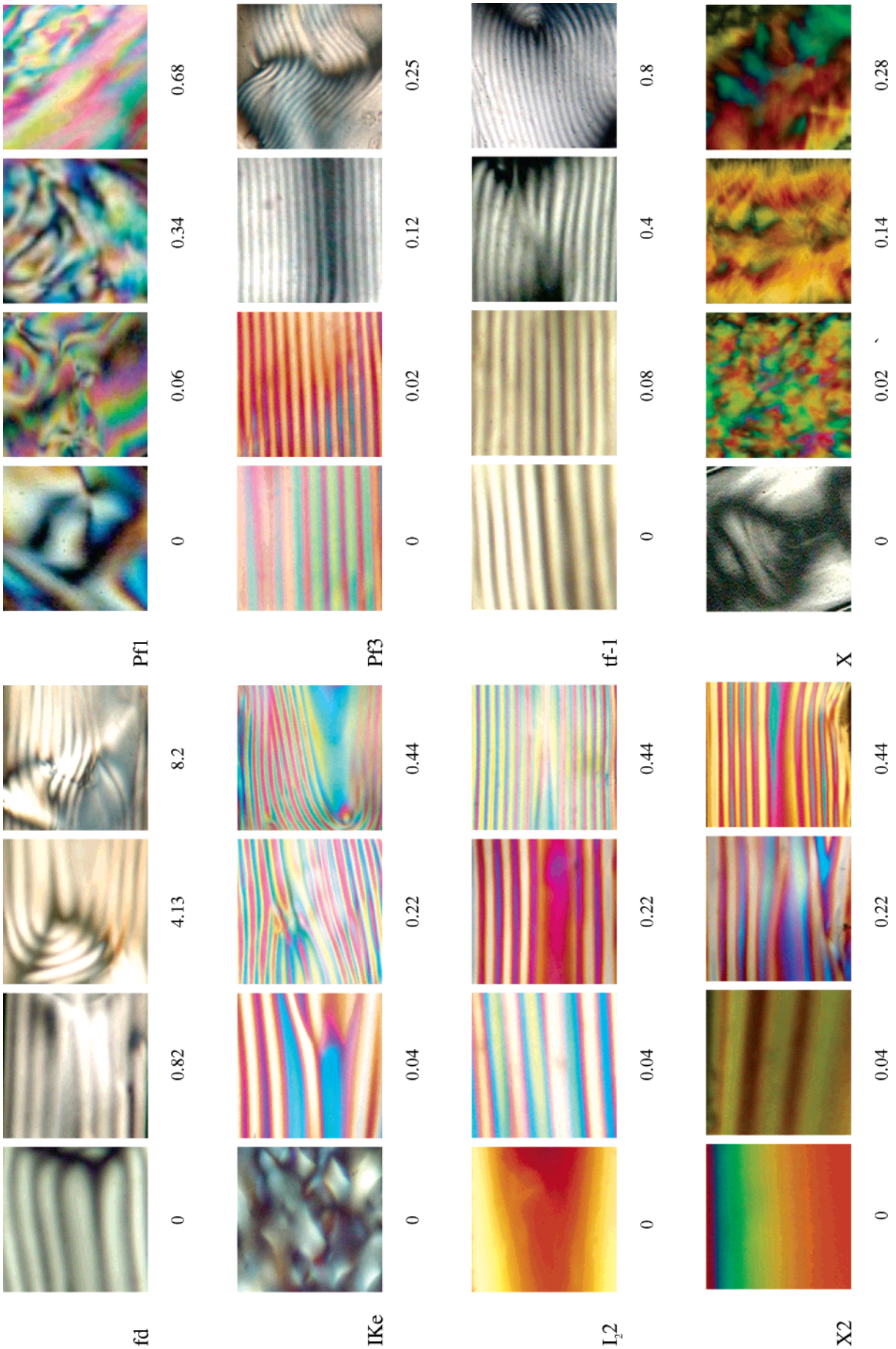

Figure 6. Effect of SDS on liquid crystal phases of eight viruses. The mole ratios of SDS per protein subunit (M_{SDS}/M_{SU}) are given under the images. The corresponding weight/volume concentrations of SDS were (fd) 0%, 0.1%, 0.5%, and 1.0%, (IKe, I_2, and X-2) 0%, 0.01%, 0.05%, and 0.1%, (Pf1) 0%, 0.01%, 0.05%, and 0.1%, (Pf3) 0%, 0.01%, 0.05%, and 0.10%, (tf-1) 0%, 0.001%, 0.005%, and 0.010%, and (X) 0%, 0.01%, 0.05%, and 0.1%. Full infectivity was retained at these levels of SDS. The side lengths of the squares correspond to 0.5 mm. For IKe, I_2, and X-2, the phases are nematic at 25 mg/mL virus in the presence and absence of SDS.

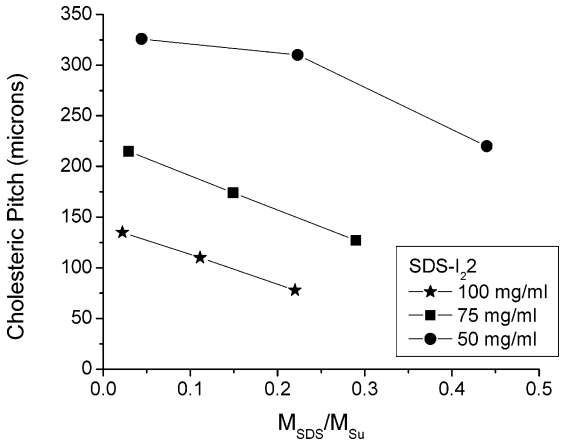

Figure 7. Effects of SDS on the liquid crystal behavior of $I_2$2 virus. $I_2$2 is nematic in the absence of any SDS. A phase change from nematic to cholesteric was observed at the lowest M_{SDS}/M_{Su} value tried for each virus concentration. Thereafter, cholesteric pitches decreased with increasing M_{SDS}/M_{Su}. Closely similar plots were obtained for IKe and X-2. Such plots for fd, Pf3, and tf-1 are also similar, but these three yield cholesteric phases in the absence of SDS.

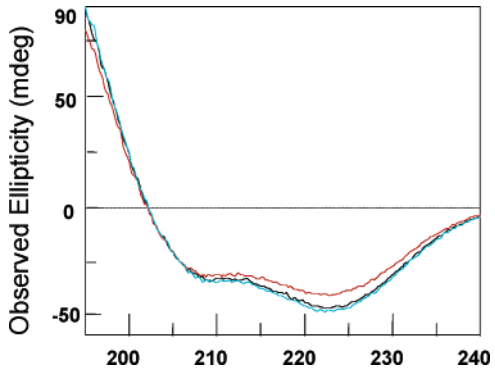

Figure 8. CD spectra of $I_2$2 at 0.2 mg/mL virus and at weight/volume SDS concentrations of 0% (lowest spectrum at 222 nm), 0.011% (middle spectrum at 222 nm), and 0.055% (highest spectrum at 222 nm). The path length was 1 mm. Increased SDS led to decreased amplitude at 222 nm without affecting the spectra above 250 nm. Similar results were obtained for all seven of the other viruses.

Unpublished observations by D. Israeli and by J. Kota (at the Public Health Research Institute) of CD spectra and phage viabilities for fd, Pf1, and X in the presence of SDS showed that the α-helical contents could be significantly reduced without affecting the DNA conformations or infectivity levels. It appeared that low levels of SDS could perturb capsid structures without perturbing the DNA structures. In this study, the prior CD results on fd, Pf1, and X were reproduced and results for the five additional phages were obtained. Figure 8 shows the CD behavior of $I_2$2, which is exemplary of that of the eight viruses and is consistent with the reduction of the α-helical content of the capsid protein.

Phage fd remained infective up to 1% SDS (w/v), whereas $I_2$2, IKe, X2, Pf1, Pf3, and X remained infective only up to 0.1% SDS. Phage tf-1 was the most delicate and showed infectivity only up to 0.01% SDS (w/v). The causes of these large differences in sensitivity to SDS are not known. As stated above, results presented in this paper are for fully infectious viruses.

The behavior of X in forming a gel and its transformation into nematic liquid crystals on addition of Ag^+ ions, Hg^{2+} ions, or SDS is a curious exception to the liquid crystal forming behavior of the other viruses. These phenomena were not expected, and we have no explanation for them.

Uniquely of all eight viruses, only Pf1 was unaffected by either the metal ions or the SDS. The nematic phase of Pf1 was maintained in the presence of either class of dopant as shown in Figure 9.

Discussion

For the six viruses fd, IKe, $I_2$2, X-2, Pf3, and tf-1, cholesteric phases arise spontaneously or can be induced (Figures 1 and 6). The pitches of the cholesteric phases of these viruses are affected in opposite directions by the presence of DNA-specific perturbants on the one hand and protein-specific structural perturbants on the other (Figures 4 and 5 and Figures 6 and 7, respectively). These observations demonstrate that the source of the liquid crystal properties arises from the way the DNA and protein helices interact, a conclusion in line with the fact that these viruses are quite similar in structure except for differences in their capsid and DNA helical symmetries, as discussed in the Introduction. Therefore, acceptance of the Meyer hypothesis[8] of large-length-scale chirality, that is, coiling, as the explanation for the differing liquid crystal results for fd and Pf1 leads to the conclusion that the ultimate determinant of the coiling behaviors of filamentous phages resides within the nature of their DNA−protein interactions.

Coiling requires subunit polymorphism. Subunits on the inside of any bend or coil are closer to one another than those on the outside. Therefore, in coiled filaments made of chemically identical subunits, the subunits are not in equivalent positions and do not have equivalent interactions with their neighboring subunits. In the well-known case of flagella, for example, the chemically identical flagellin subunits are forced into different structural states by molecular motors at the cell proximal end to generate coiling.[30−32] In contrast, we propose here that filamentous phage coiling stems from forces internal to the filament. These internal forces make the structural states of the chemically identical subunits in the virions inherently different; that is, the environment about the subunits will vary along the filament length. This establishes inherently the necessary condition for a virion to deviate from straightness. If the differing states are periodic, the overall shape can be that of a coil.

Existing structural information on the six phages that give rise to cholesteric liquid crystals is consistent with nonequivalent capsid protein subunits. The parameters for fd provide a specific example. The DNA helix in fd has an average nucleotide rise of 2.8−3.0 Å and a pitch of 28−30 Å depending on the conditions.[4,17,33] As described above, the helical sense is right handed and the bases are stacked and hydrogen bonded, but only a fraction (about 25%) of the H-bonding can be of the Watson−Crick type because the opposing bases in the antiparallel strands can be any of the four except within a small base-paired packaging signal hairpin at one end. The average nucleotides-per-subunit ratio in fd is very close to 2.4.[4,34] Should the ratio be exactly 2.4, there would be 12 nucleotides in each

(30) Asakura, S. *Adv. Biophys.* **1970**, *1*, 99−155.
(31) Berg, H. C.; Anderson, R. A. *Nature* **1973**, *245*, 380−382.
(32) Kitao, A.; Yonekura, K.; Maki-Yonekura, S.; Samatey, F. A.; Imada, K.; Namba, K. *Proc. Natl. Acad. Sci. U.S.A.* **2006**, *103*, 4894−4899.
(33) Marzec, C. J.; Day, L. A. *Biophys. J.* **1983**, *42*, 171−180.
(34) Marzec, C. J.; Day, L. A. *Biophys. J.* **1994**, *67*, 2205−2222.

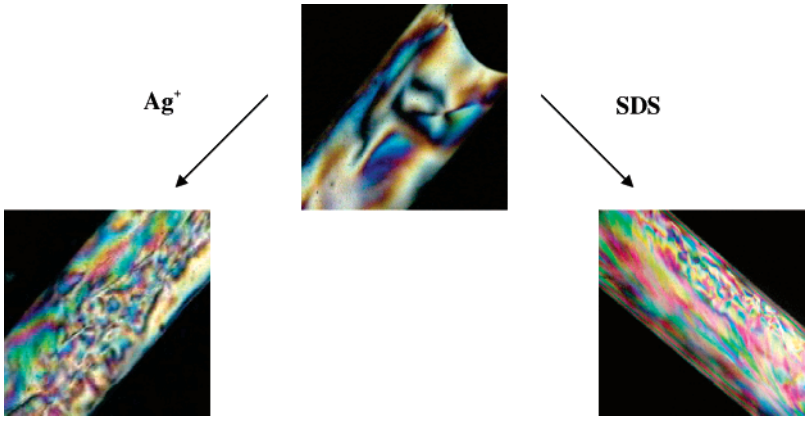

Figure 9. Nematic liquid crystals of Pf1 at 25 mg/mL in 0.15 M borate buffer in the absence of dopants (top) and in the presence of Ag^+ at $M_{Ag^+}/M_{Nu} = 0.6$ (left, from Figure 3) and in the presence of SDS at $M_{SDS}/M_{Su} = 0.68$ (0.1% (w/v) SDS).

strand contacting 10 subunits in the 2 pentamers of the approximate capsid repeat. Because the helical symmetries of the capsid and DNA differ, each of the 24 nucleotides has a different contact point on the individual subunits within these 10 protein subunits.[33,34] The differing DNA contact points make the fd subunits nonequivalent. Similarly, the IKe, $I_2$2, and X-2 subunits in their class I capsids must exist in multiple microstates as a consequence of the same type of differences between DNA and capsid symmetries as for fd. The same arguments hold for virions with capsids of any symmetry type if the pitches of the DNA and capsid are not the same and/or if the stoichiometric ratio of nucleotides per subunit has a noninteger value. Given that tf-1 and Pf3 form cholesteric liquid crystals, one or both of these conditions must hold for each of these two viruses.

Pf1 is unique among the eight virions in forming a nematic phase that is maintained (Figure 9) under conditions of added dopants under which the liquid crystal properties of all the other phages are affected. Pf1 is also unique among the eight virions in having a 1:1 stoichiometric ratio of nucleotides to protein subunits.[4,22,35] This unit stoichiometry is the basis for a Pf1 structure model in which the pitches of the DNA and capsid helices are the same and in which the protein subunits all point in the same direction (e.g., "up") and every other subunit interacts with an "up"-strand nucleotide while the alternate subunits interact with "down"-strand nucleotides, giving two nonequivalent subunit structures.[22] This Pf1 model with equivalent DNA and capsid helical pitches and phases is consistent with a filament absent of any polymorphism that might lead to regular deviation from straightness, both in the presence and in the absence of the metal ion or SDS dopants. The model is therefore consistent with its liquid crystal behavior. A recent assignment of 93% of the 251 carbon and nitrogen atoms in the Pf1 subunit to resonances in its magic angle spinning solid-state NMR spectra (MAS NMR) has indicated just one type of subunit conformation in Pf1 in its high-temperature form, with multiple chemical shifts observed at only two amino acid residues.[36] The observations are consistent with Pf1 having two nonequivalent subunit microstates. Also the DNA structure in this matching, with its high twist and axial rise,[22] is consistent with the results of single-molecule physics experiments that generate P-form DNA,[25] with the results of polarized vibrational spectral data for oriented Pf1 specimens,[37] and with electrostatic theory.[34]

Pf3 has an X-ray fiber diffraction pattern that is very similar to that of Pf1,[23] and both viruses have been proposed to have DNAs with pitches equal to their capsid pitch and with bases directed outward.[4,22,31−33] Yet liquid crystals of Pf3 are cholesteric, while those of Pf1 are nematic. The critical difference is in their rise-per-nucleotide values, 5.8 Å in Pf1 but only 2.4 Å in Pf3, corresponding to nucleotide:subunit ratios of 1 (unity) for Pf1 and about 2.5 for Pf3.[4] The noninteger stoichiometry of Pf3 calls for many more than two nonequivalent subunit microstates. Our observation of cholesteric liquid crystals for Pf3 indicates a large-length-scale chirality arising from this polymorphism.

The increase in apparent coiling induced by SDS manifested by the cholesteric phases for IKe, $I_2$2, and X-2 and the tightened cholesteric pitches for fd, tf-1, and Pf3 (Figure 6) is consistent with the surfactant penetrating into the hydrophobic regions between the individual capsid protein units. In general the capsid structure tends to be straight, and the tighter and stronger the packing between subunits in the capsid the greater the tendency of the filament to resist coiling. Since the α-helicity of the capsid proteins arises from both the primary structure of the protein and the packing of the proteins, reduction of the α-helicity can be expected on surfactant penetration. This reduction in α-helicity is demonstrated by the reduced ellipticity amplitudes at 222 nm correlated with the addition of SDS (Figure 8).[24] The addition of SDS therefore apparently allows a "softening" of the capsid structure, allowing subunit nonequivalence to give rise to deformation of the filament. This softening of the capsid structure then allows enhanced coiling, giving rise to lower cholesteric pitches in already existing cholesteric liquid crystals, or the transformation of a nematic to a cholesteric state, consistent with the experimental observations (Figures 6 and 7). On the other hand, the liquid crystal changes caused by the metal ions, although not predictable, require a weakening of the DNA−capsid interactions and therefore a lessening of protein structural polymorphism, leading to a reduction in coiling. Although we cannot demonstrate this directly from the data available here or in the literature,[29] an alternate or

(35) Kostrikis, L. G.; Liu, D. J.; Day, L. A. *Biochemistry* **1994**, *33*, 1694−1703.
(36) Goldbourt, A.; Gross, B.; Day, L. A.; McDermott, A. E. *J. Am. Chem. Soc.*, in press.
(37) Tsuboi, M.; Kubo, Y.; Ikeda, T.; Overman, S. A.; Osman, O.; Thomas, G. J., Jr. *Biochemistry* **2003**, *42*, 940−950.

concomitant effect of the metal ions may be to stiffen the DNA, hence reducing the chiral flexing.

Considerations from the standpoints of geometry and electrostatics have elucidated how nonequivalent protein subunit structures can derive from periodic nonequivalent interactions between the capsids and DNAs in filamentous phages.[33,34] Such analyses can be used to explore how periodic subunit polymorphism so derived could result in large-length-scale coiling. In this coiling the left- and right-handedness must be related diastereomerically as a consequence of the local chirality of the filament, and therefore, the populations of left- and right-handed coils may be unequal. The conditions for formation of a cholesteric liquid crystal phase would thus be satisfied.[10,11]

The evidence obtained here assigned to subtle aspects of phage morphology that are amplified by the nature of their liquid crystals has ramifications for various structural methods and gives direction to further studies. For example, subunit polymorphism derived from DNA−capsid interactions in many filamentous phages would point to inherent restrictions on the ways fiber diffraction data are used in developing detailed structure models. Fiber diffraction data have provided key information on capsid symmetries and subunit conformations, but the present results raise questions as to how different parts of a capsid contribute to the diffraction patterns. Those phages that exhibit cholesteric liquid crystal phases are thereby exhibiting subunit structural polymorphism that may affect the side chain and backbone groups of several amino acid residues. Evidence of polymorphism in a recent study of fd by cryoelectron microscopy may derive in part from the DNA−capsid interactions.[17] It is expected that MAS NMR will allow the elucidation of the atoms affected by the polymorphism in other filamentous phages. It may be possible to obtain direct correlations of length scales of coiling and liquid crystal behavior through studies of these systems by electron microscopy and dynamic light scattering. In any case, liquid crystal methods, which least perturb the overall structure and hence internal structure, have been found to be useful in detecting inherent subunit polymorphism.

Acknowledgment. We are grateful to the late Murray Goodman for encouraging M.M.G. and L.A.D. to undertake collaborations on filamentous phages. We thank Seth Fraden of Brandeis University for many helpful discussions and technical suggestions and Lenny Mindich of the Public Health Research Institute and Neville Kallenbach of New York University for their interest and encouragement throughout this study. We thank David E. Bradley of St. Johns University, Newfoundland, for providing our original stocks of phages X-2, X, and tf-1. We also thank Robert Donnelly of the University of Medicine and Dentistry of New Jersey, Jay Newman of Union College, and Joseph S. Wall of the Brookhaven National Laboratory for discussions and help with characterizations of some of the viruses used in this study to be reported separately. The research was financially supported by funds from the Public Health Research Institute (L.A.D.) and by grants from the Polymers and Chemistry Programs of the National Science Foundation and from the Petroleum Research Fund, administered by the American Chemical Society (M.M.G). We are grateful to these organizations and to the Othmer Institute for Interdisciplinary Studies at the Polytechnic University for initial support. The work reported is taken in part from the doctoral thesis of S.T. at the Polytechnic University.

JA068498D